JJEE
Volume 2, Number 2, 2016
Pages 160-171
Jordan Journal of Electrical Engineering
ISSN (Print): 2409-9600, ISSN (Online): 2409-9619

Thorough Investigation of BER Simulation of DPSK in Underwater Acoustic Channel

Aser M. Matarneh

Department of Electrical Engineering, Mu'tah University, Al-Karak, Jordan
e-mail: aser.matarneh@mutah.edu.jo

Received: February 13, 2016 *Accepted: March 9, 2016*

Abstract— This paper presents performance evaluation of differential quadrature phase shift keying (DQPSK) transmission over underwater acoustic channel (UWA). In this paper, a channel model that simulates the multipath fading characteristics of the shallow underwater channel is carried out in order to make possible of performance evaluation of DQPSK transmission. Next, a single carrier DQPSK communication with convolutional encoder is simulated and carried out. The impact of channel capacity is explored as well. The system performance will be measured by the bit error ratio (BER). Investigations of multipaths and transmission distance will be obtained and discussed in details.

Keywords— Ambient noise, BER, Channel capacity, Convolutional coding, DQPSK, Multipath, SNR, Underwater acoustic channel.

I. INTRODUCTION

The wideband underwater acoustic communication is one of the most severe channels in terms of time- dispersive and frequency selectivity. The large delay spread exhibited comes from the fact that the available bandwidth is limited by frequency-dependent ambient noise and path loss which is also a function of frequency and low speed of sound in water. Design and simulation of UWA communication systems require accurate channel modeling in order to be able to explore the channel dynamics and statistical description of the random channel variations in time [1]-[4].

Some applications are not limited to UWA system such as oil industry, pollution monitoring in environmental systems, remote control, collection of scientific data recorded at ocean bottom stations, speech transmission between divers, mapping of the ocean floor, detection of objects and discovery of new resources [4]-[6].

Signal propagation in underwater acoustic channel encounters many issues which make the signal fluctuate randomly [6], [7]. First, frequency-dependent attenuation due to the absorption of the acoustic waves in water limits the transmission distance. Second, low propagation speed of the sound is roughly around 1500m/s. Third, multipath due to the reflection from the bottom and surface of sea causes echoes and interference [6], [7].

There has been numerous modeling of acoustic channel which attempts to account for channel physics. Such channel modeling has been directed towards channel characteristics, signal quality and system performance. Naturally, underwater acoustic channel is a typical high BER channel characterized by poor communication quality and high propagation delay. Channel coding can reduce the BER effectively at the cost of some communication bandwidth loss [6], [8]. Moreover, phase tracking modulation schemes can also improve the resilience of the system and the system quality.

The advantage of using differentially encoded PSK (DPSK) with differentially coherent detection is the simple carrier recovery it allows albeit at 3dB performance losses compared with coherent detection [6], [9]. Differentially coherent detection alleviates the need for

Corresponding author's e-mail: aser.matarneh@mutah.edu.jo

channel estimation and uses simple carrier recovery. Unlike coherent detection, DPSK does not require an equalizer and thus reduces the receiver complexity [10]. However, it does rely on channel invariance. If there is perfect channel knowledge, differential detection will exhibit some penalty in the performance (around 3dB loss in DPSK compared to PSK). If the channel estimation is not accurate, differential detection becomes competitive or even superior to coherent detection, where the performance of coherent detection degrades accordingly. This fact has been observed in both wireless radio and optical channels.

DPSK encodes information in the signal phase relative to the previous symbol rather than to an arbitrary fixed reference; and may be referred to as a partially coherent modulation. As with PSK, one can use an array of M distinct levels (M-DPSK). While this strategy substantially alleviates the carrier phase-tracking requirements, the penalty is an increase in error probability over PSK at an equivalent data rate [11].

A well-known class of error-correction codes, convolutional codes, has been favored in many communication systems such as optical fiber communication and wireless communication systems. Convolutional codes have many attractive features such as simple encoding and decoding process. The decoding process is based on either hard decision or soft decision algorithms of Viterbi detection, which continuously handles bit streams and eliminates buffering and synchronization issues. However, a penalty is the increase of the occupied bandwidth due to the coding gain incorporated. This method of differential encoding is also less resilient to the effects of oscillator phase noise, which is a very important consideration in millimeter-wave systems [11].

The paper is organized as follows; the mathematical model of the underwater acoustic channel is presented in section II. The ambient noise is given in section III. Section IV discusses the simulation results of channel capacity, bandwidth efficiency and single carrier DQPSK communication with convolutional encoder. The system performance results are introduced in terms of BER. Then, the conclusion is drawn.

II. MATHEMATICAL MODEL FOR UWA

Path loss of an underwater acoustic communication channel depends on the transmission distance and signal frequency. The acoustic path loss is represented as follows [12]:

$$A(l, f) = A_0 l^k \alpha(f)^l \tag{1}$$

Where A_0 is a unit-normalizing constant; k is the spreading factor; and $\alpha(f)$ is the absorption coefficient.

The absorption coefficient can be expressed using Thorp's empirical formula [13], [14]:

$$\alpha(f) = 0.11\frac{f^2}{1+f^2} + 44\frac{f^2}{4100+f^2} + 2.75\times10^{-4} f^2 + 0.003 \tag{2}$$

Where f is given in kHz; and the absorption coefficient is given in dB/km. For every path, the attenuation and cumulative reflection coefficient are calculated individually before they are summed together. Therefore, the overall transfer function of the UWA channel in the frequency domain can be described as follows [15]:

$$H(l,f)=\sum_{p=0}^{P-1}\frac{\Gamma_p}{\sqrt{A(l_p,f)}}e^{-j2\pi f\tau_p} \tag{3}$$

$\tau_p = l_p / c$ is the path delay, and c is the nominal speed of the sound underwater (1500m/s). The propagation paths each of length l_p, p =0,…P-1. Γ_p models additional losses incurred on the p^{th} path (e.g. cumulative reflection loss) and is defined as follows:

$$\Gamma_b = \gamma_s^{n_{sp}} \gamma_p^{n_{bp}}(\theta_p) \tag{4}$$

Where γ_s is the surface reflection coefficient; and γ_p is the bottom reflection coefficient. θ_p is the grazing angle (the angle between the received signal and the horizontal axis) associated with the p^{th} propagation path. n_{sp} *and* n_{bp} are the number of surface and bottom reflections, respectively. Each bottom reflection is modeled by a coefficient $\gamma_b(\theta)$ [13], [16]:

$$\gamma_b(\theta)=\begin{cases}\dfrac{\rho_b\sin(\theta)-\rho\sqrt{(c/c_b)^2-\cos^2(\theta)}}{\rho_b\sin(\theta)+\rho\sqrt{(c/c_b)^2-\cos^2(\theta)}}, & \cos(\theta)\le c/c_b \\ 1, & \text{otherwise}\end{cases} \tag{5}$$

Where ρ and c are the density and speed of sound in water respectively. ρ_b and c_b are the density and speed of sound in bottom.

The speed of sound in water is limited between 1450m/s and 1540m/s, whereas the nominal sound speed is 1500m/s. However, some small variations take place because of the sound velocity in the UWA channel which results from temperature changes and Hydrostatic pressure.

III. NOISE CONSIDERATIONS IN UWA

It should be pointed out that high frequency signals in UWC exhibit a much stronger attenuation than the lower frequency signals for each propagation path. However, underwater noise is primarily high for low frequencies which limit using high signal frequencies to avoid noise frequency bands. Therefore, a compromise between signal attenuation and ambient noise is necessary to decide which frequency band to consider [12]. There are several types of noise or ambient noise in the underwater environment. The acoustic channel noise can be described as the sum of each parts:

A. Turbulence Noise

Turbulence noise effect can be significant in very low frequencies less than 10 Hz. It can be modeled as in [14], [17]:

$$10\log N_t(f) = 17 - 30\log(f) \tag{6}$$

Where N_t denotes turbulence noise.

B. Shipping Noise

Its effect can be noticed in a frequency range of 10-100Hz [12], [14]:

$$10 \log N_s(f) = 40 + 20(s - 0.5) + 26 \log(f) - 60 \log(f + 0.03) \quad (7)$$

Where s is the shipping activity factor that ranges between 0 and 1.
Wave and other surface motion caused by wind and rain is a major factor in the mid frequency region of 100–1000Hz [12], [14], [15]:

$$10 \log N_w(f) = 50 + 7.5\sqrt{w} + 20 \log(f) - 40 \log(f + 0.4) \quad (8)$$

Where w is the wind speed in m/s.

C. Thermal Noise

It is significantly above 100kHz [12], [17], [18]:

$$10 \log N_{th}(f) = 20 \log(f) - 15 \quad (9)$$

The overall combined ambient noise in UWA is given by [14]:

$$N(f) = N_t(f) + N_s(f) + N_w(f) + N_{th}(f) \quad (10)$$

For the empirical equations above, dB re μPa per Hz is given as a function of frequency in kHz. There are two possible procedures that can be followed to evaluate the BER versus the *SNR*. First, the transmitted power depends on the distance between the transmitter and the receiver; therefore, the *SNR* can be fixed at the desired value before the transmitted power will be evaluated. Another way is to fix the transmitted power and calculate the *SNR* based on the equation below [12], [15]. The latter is used throughout this paper, and the transmitted power is fixed at $2x10^6$ dB re μPa.

$$SNR(l, f) = \frac{P / A(l, f)}{N(f)\Delta f} \quad (11)$$

The transmission bandwidth $B(l)$ is defined as the range of frequencies around optimal frequency $f_o(l)$ for which $SNR(l, f) > SNR(l, f_o(l))/2$. The *SNR* becomes:

$$SNR(l, B(l)) = K_l \frac{\int_{B(l)} S_l(f) A^{-1}(l, f) df}{\int_{B(l)} N(f) df} - 1 \quad (12)$$

Where K_l is a constant, whose value is to be determined. P is the transmitted power; Δf is the receiver noise bandwidth (a narrow band around the frequency f). The AN product, $A(l, f)$ $N(f)$, determines the frequency-dependent part of the *SNR*.

When the 3dB bandwidth, $B_3(l)$ (around optimal frequency where the product of AN is minimum), is used, the corresponding transmission power is determined [12], [15]:

$$P_3(l) = SNR_0 B_3(l) \frac{\int_{B_3(l)} N(f)}{\int_{B_3(l)} A^{-1}(l,f)} \tag{13}$$

Where SNR_0 is the desired threshold SNR.

The power spectral density (*p.s.d*) of the transmitted signal is flat, $S(l,f) = S_l$ for $f \in B(l)$, and 0 elsewhere. The optimal energy distribution S_l is given by:

$$S_l(f) = \begin{cases} K_l - A(l,f)N(f) & f \in B(l) \\ 0 & \text{elsewhere} \end{cases} \tag{14}$$

Finally, the channel capacity can be described as follows [12]:

$$C(l) = \sum_i \Delta f \log_2 \left[1 + \frac{S_l(f_i) A^{-1}(l,f_i)}{N(f_i)} \right] \tag{15}$$

Before proceeding iteratively in the simulation, the desired SNR_0 needs to be fixed; and the 3dB bandwidth $B_3(l)$ needs to be calculated for each distance. The initial value of K_l will start from a value equal to AN_{min}. The rest of algorithm procedure is described as follows:

1. Calculate $SNR(n)$ from (12) using the bandwidth $B(n)(l)$ and the constant $K_l(n)$.
2. The resulting $SNR(n)$ will be compared to SNR_0. If $SNR(n) < SNR_0$, K_l will be increased by a small amount, and the procedure will continue.
3. Whenever $SNR(n)$ reaches (or slightly exceeds) SNR_0, the procedure ends. The current value of $K_l(n)$ is set as the desired constant K_l; and the resultant value of the bandwidth $B(n)(l)$ is set as the desired bandwidth $B(l)$. The optimal energy distribution and channel capacity are then calculated by using (14) and (15) respectively.
4. The procedure is repeated for every desired SNR_0 for BER evaluation at various distances and different multipaths.

It should be mentioned that in underwater acoustic channel, the sound speed variation with depth is mostly evident in deep water channels. However, sound speed c in shallow water (< 100m deep) can be considered constant; path lengths can be calculated using plain geometry; and path delays can be obtained as lp/c.

The proposed channel model, as shown in Fig. 1, considers a fixed transmitter and receiver placed near the bottom at a depth of 75m (shallow water) and separated by variable distances starting from 3km. The practical spreading factor is taken to be k= 1.5, with no wind (i.e. w=0) and shipping factor s=0.5. Table 1 summarizes all the parameters needed to carry out the channel model.

TABLE 1
UWA PARAMETERS

Parameter	Value
Spreading factor k	1.5
Wind speed w	0
Shipping activity s	0.5
ρ	1000g/m^3
c	1500m/s
ρ_b	1800g/m^3
c_b	1300m/s
n_{sp}	1
n_{bp}	1
γ_s	-1

Regarding multipath effect, up to six paths including the shortest path are considered. The total multipath spread is dominated by the longest path delay, which is on the order of tens of ms. As a simple case study, relative delays to the shortest path are taken as: 10, 20, 40, 60, and 80ms, respectively.

The implementation process of Coded-DQPSK-UWA model is shown in Fig. 2 and summarized as follows:

- The data bits are convolutionally encoded with a code rate ½, generator polynomial $(133,171)_8$, and constraint length 7.
- The encoded bits are mapped into in-phase and quadrature components of the complex symbol using Gray-coded mappings, and are modulated by DQPSK.
- The UWA channel is assumed to be stationary channel for, at least, the transmission of one symbol. Also, noise is considered as an ambient noise.
- At the receiver, demodulation is carried out. Then, the decoding process employs the soft-decision Viterbi decoding algorithm which involves Maximum Likelihood Ratio (MLR) as soft-bit metrics.
- The recovered data bits are compared with transmitted bits for BER calculations. It should be noted that around 160,000 bits have been taken for each iteration of errors collection.

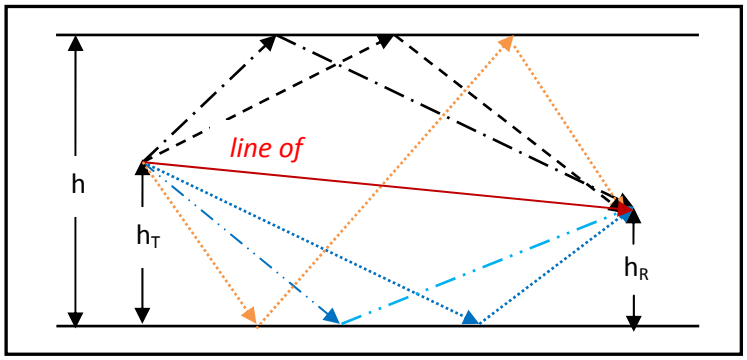

Fig. 1. Proposed UWA channel model

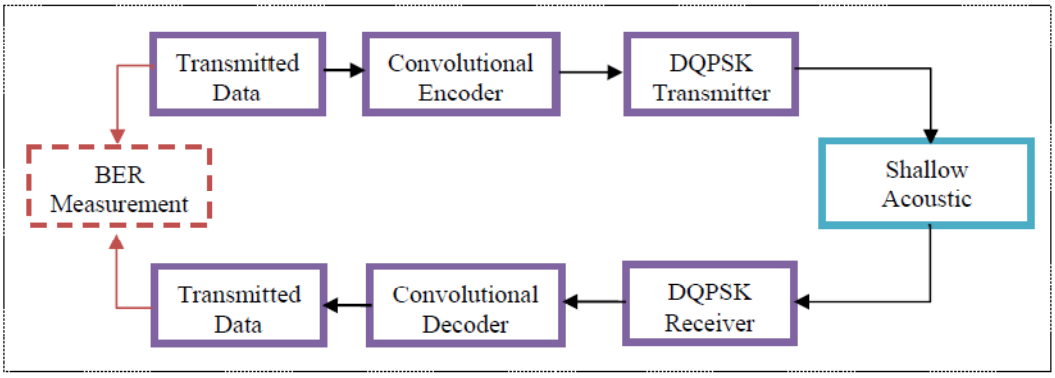

Fig. 2. System block diagram

IV. RESULTS AND DISCUSSIONS

Transmitted signal *p.s.d.* for various distances and threshold *SNR* of 20dB is shown in Fig. 3. It can be seen that the transmitted signal *p.s.d.* is flat for the region below the cut-off frequency. In other words, $S(l, f) = Sl$ for $f \in B(l)$, and zero elsewhere. Furthermore, it is noteworthy that by increasing the distance, the cut-off frequency decreases at fixed *SNR*. Fig. 3 indicates that the 3dB available bandwidth is reduced for longer distances.

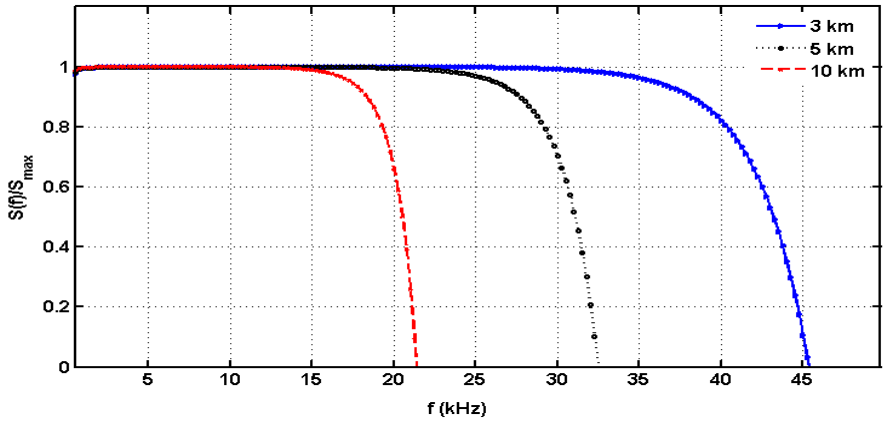

Fig. 3. Transmitted signal *p.s.d.* for various distances and threshold *SNR* of 20dB

The effect of varying *SNR* on the link capacity and bandwidth is presented in Fig. 4. Shown in the figure is the bandwidth efficiency, i.e. the ratio between the system capacity and bandwidth, $C(l)/B(l)$ in bps/Hz, for several values of transmission distance, $l = 3$, 5, and 10km. It can be noted that the bandwidth efficiency decreases as the distance increases. Such decrease is almost constant within the range of *SNR* taken between 0-30dB.

In order to validate the simulated model of signal transmission over UWA, Fig. 5 demonstrates the results of both QPSK and DQPSK transmitted over UWA with 3km separation distance between transmitter and receiver considering five multipaths. It clearly show the superiority of QPSK of around 3dB over DQPSK. Such penalty is reported in [19] and depicted here to validate the simulation model carried out by MATLAB.

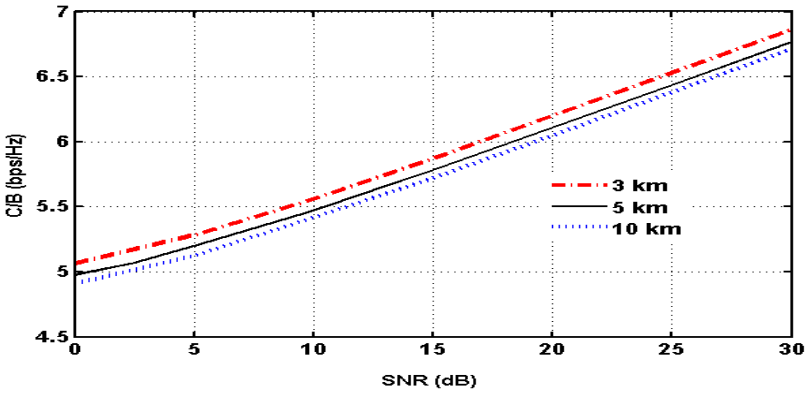

Fig. 4. Bandwidth efficiency for various distances

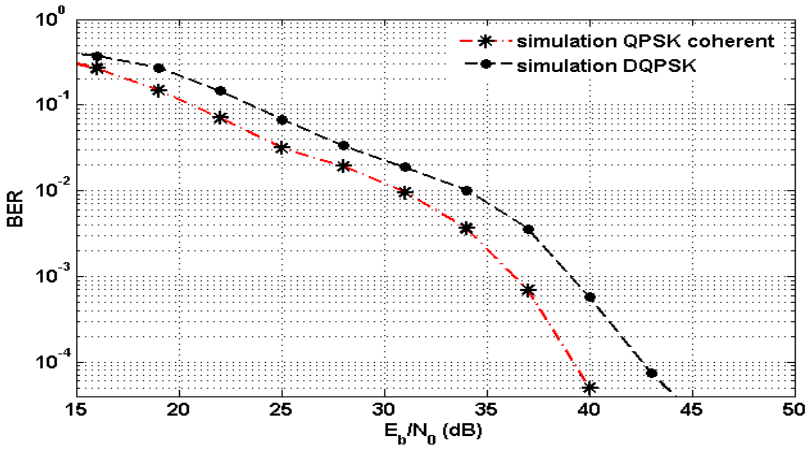

Fig. 5. Comparison between QPSK and DQPSK over 3km distance

The superiority of using convolutional coding is depicted in Fig. 6. Both uncoded-QPSK and coded-QPSK are shown in the figure for a transmission distance of 3km and consideration of a single path. It can be noted that around 2dB gain is achieved when using convolutional coding at BER of 10^{-6}.

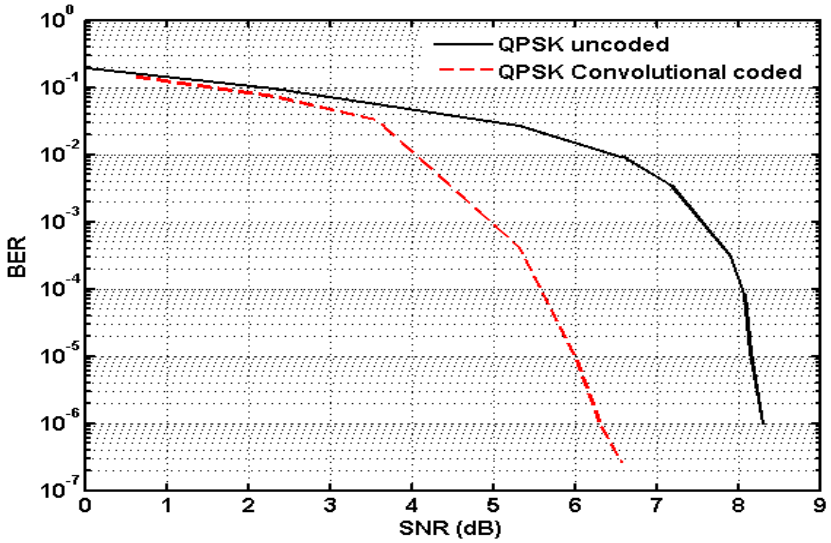

Fig. 6. Comparison between uncoded-QPSK and coded-QPSK over 3km distance

To recognize the challenges imposed by transmission distance and multipaths, Figs. 7-10 explain the transmission distance effect when using QPSK (Fig. 7), and DQPSK (Figs. 8-10), respectively.

It is clear that the performance of single path channel outperforms three or six paths in both coherent and differential coherent transmission over UWA. However, based on Fig. 7 and Fig. 8, which compare the three multipaths case at BER of 10^{-6}, the QPSK is superior to DQPSK by around 5.5dB. For six-multipath case, the QPSK underperforms the DQPSK by 1dB at 10^{-4}; and an error floor starts to appear after *SNR* of around 40dB as increasing the average *SNR* does not improve the system. For higher multipaths, the DQPSK still plays better and becomes robust to the time and frequency spreading of the channel because it can track phase changes properly.

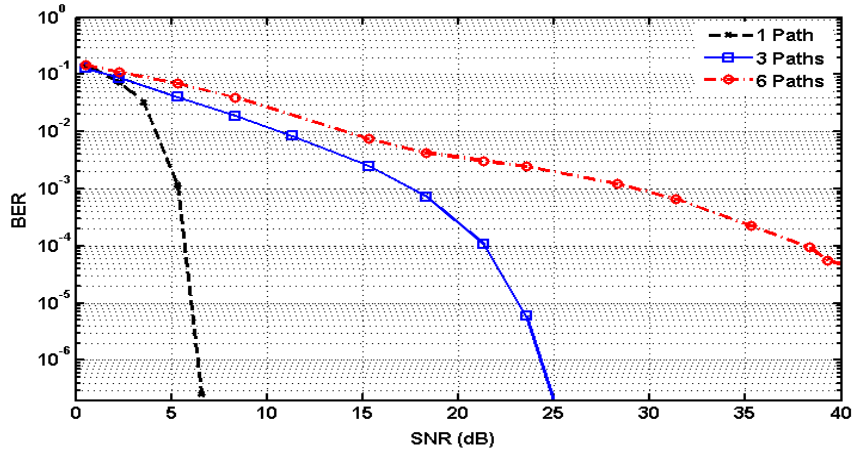

Fig. 7. QPSK transmission performance over UWA with different paths and distance 3km

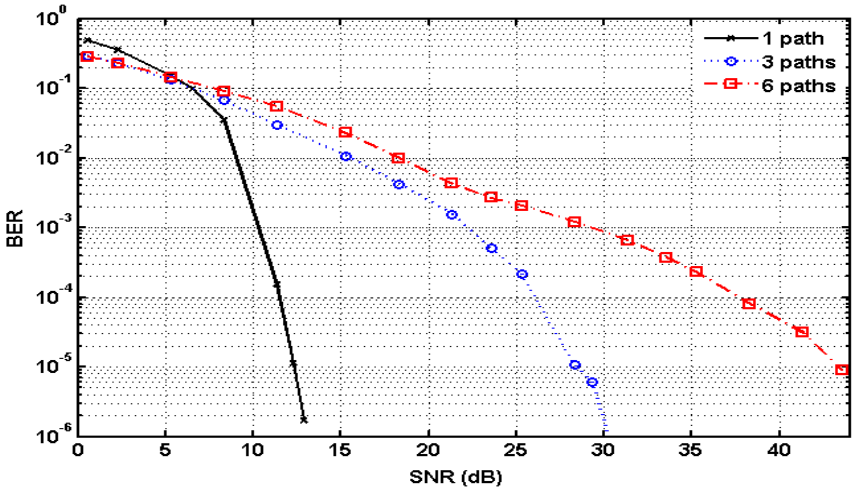

Fig. 8. DQPSK transmission performance over UWA with different paths and distance 3km

At transmission distance of 5km, Fig. 9 shows that the three and six paths start to diverge by greater than 3dB at BER of 10^{-3}. Moreover, at BER of 10^{-5}, around 12.5dB penalty is incurred of *SNR* to increase the number of paths from a single path to three paths.

For a longer distance, 10km, as shown in Fig. 10, it is worth noting that the performance of one path outperforms the three multipaths by around 17dB at BER of 10^{-6} analogous to what can be expected. It is interesting to notice that the curves of three and six paths are getting

closer as the distance increases, meaning to severe performance deterioration. Hence, the distance effect becomes clearly much stronger than the multipath effect.

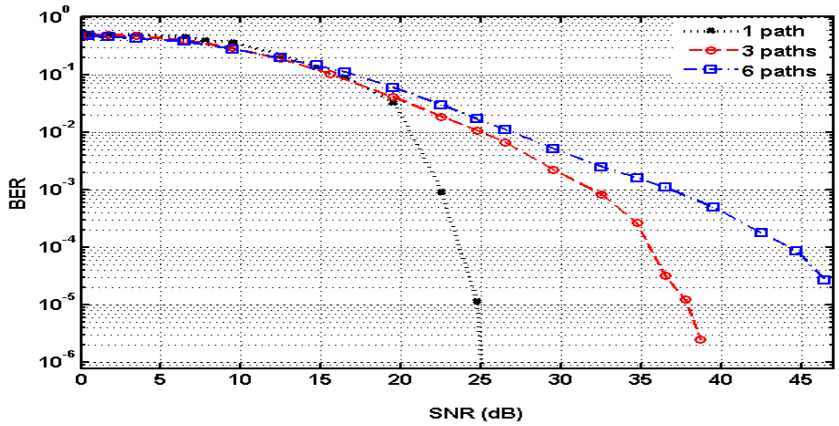

Fig. 9. DQPSK transmission performance over UWA with different paths and distance 5km

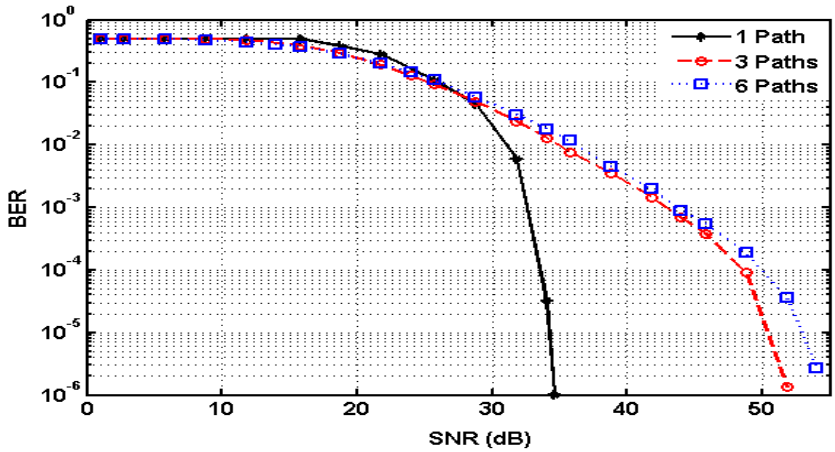

Fig. 10. DQPSK transmission performance over UWA with different paths and distance 10km

In Fig. 11, the effect of the transmission distance on the system performance can be observed for different distances 3, 5, and 10km, respectively. Considering three multipaths, the 5km curve is 9.42dB away from the 3km curve at BER 10^{-5}. Furthermore, the 10km curve shows a large need of *SNR* to maintain the same BER for 3km curve (14dB from 5km curve at 10^{-5}).

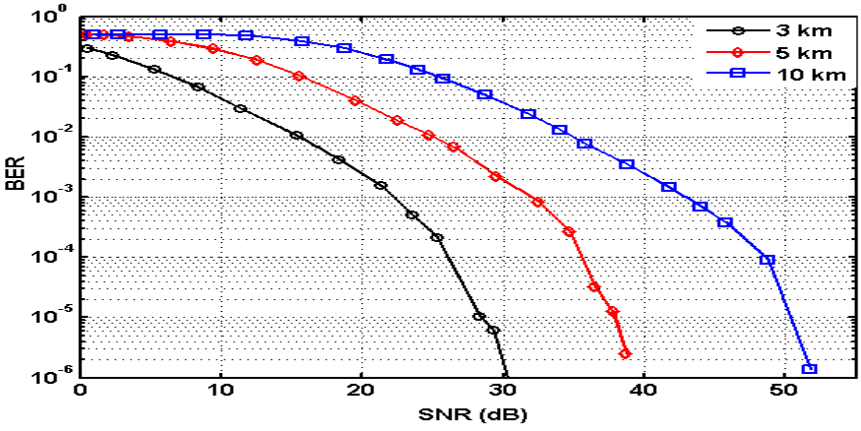

Fig. 11. Transmission distance effect for DPSK with three multipaths

V. CONCLUSION

A comprehensive model of UWA channel has been presented; the capacity, bandwidth efficiency and transmission performance of convolutionally coded DQPSK have been introduced. Moreover, the impacts of both the transmission distance effect and multipath effect have been thoroughly investigated. Future work would evaluate different kinds of coding and modulation formats for better performance and simplicity. The feasibility of image transmission as well as improvement of the throughput would also become a potential choice. In any cases, trade-off between bandwidth efficiency and system complexity needs to be considered for reliable UWA based systems.

REFERENCES

[1] Stojanovic M., "Underwater acoustic communication channels: propagation models and statistical characterization," *IEEE Communications Magazine*, vol. 47, no.1, pp. 84-89, 2009.

[2] P. Hursky, M. B. Porter, M. Siderius and V. K. McDonald, "Point-to-point underwater acoustic communications using spread-spectrum passive phase conjugation," *Journal of the Acoustical Society of America*, vol. 120, no. 1, pp. 247-257, 2006.

[3] T. J. Hajenko and C. R. Benson, "The high frequency underwater acoustic channel," *Proceedings of IEEE OCEANS Conference*, pp. 1-3, 2010.

[4] A. Caiti, E. Crisostomi and A. Munafò, "Physical characterization of acoustic communication channel properties in underwater mobile sensor networks," *Sensor Systems and Software*, vol. 24, pp. 111-126, 2009.

[5] Y. Li, X. Sha and K. Wang, "Hybrid carrier communication with partial fft demodulation over underwater acoustic channels," *IEEE Communications Letters*, vol. 17, no. 12, pp. 2260-2263, 2013.

[6] H. Esmaiel, and D. Jiang, "Review article: multicarrier communication for underwater acoustic channel," *Communications, Network and System Sciences*, vol. 6, no. 8, pp. 371-376, 2013.

[7] M. Chitre, S. Shahabudeen, L. Freitag and M. Stojanovic, "Recent advances in underwater acoustic communications & networking," *Proceedings of IEEE OCEANS Conference*, pp. 1-10, 2008.

[8] J. Trubuil, A. Goalic and N. Beuzelin, "An overview of channel coding for underwater acoustic communications," *Proceedings of IEEE Military Communications Conference*, pp. 1-7, 2012.

[9] B. J. Dixon, R. D. Pollard and S. Iezekiel, "Orthogonal frequency-division multiplexing in wireless communication systems with multimode fiber feeds," *IEEE Transacion on Microwave Theory and Technigues*, vol. 49, no. 8, pp. 1404-1409, 2001.

[10] Y. M. Aval and M. Stojanovic, "Differentially coherent multichannel detection of acoustic OFDM signals," *IEEE Journal of Oceanic Engineering*, vol. 40, no. 2, pp. 251-268, 2015.

[11] D. B. Kilfoyle and A. B. Baggeroer, "The state of the art in underwater acoustic telemetry," *IEEE Journal of Oceanic Engineering*, vol. 25, no. 1, pp. 4-27, 2000.

[12] M. Stojanovic, "On the relationship between capacity and distance in an underwater acoustic communication channel," *Proceedings of ACM International Workshop On Underwater Networks*, pp. 41-47, 2006.

[13] P. Qarabaqi and M. Stojanovic, "Statistical characterization and computationally efficient modeling of a class of underwater acoustic communication channels," *IEEE Journal of Oceanic Engineering*, vol. 38, no. 4, pp. 701-716, 2013.

[14] A. Stefanov and M. Stojanovic, "Design and performance analysis of underwater acoustic networks," *IEEE Journal on Selected Areas in Communications*, vol. 29, no. 10, pp. 2012-2021, 2011.

[15] D. E. Lucani, M. Stojanovic and M. Médard, "On the relationship between transmission power and capacity of an underwater acoustic communication channel," *Proceedings of IEEE OCEANS Conference*, pp. 1-6, 2008.

[16] L. M. Brekhovskikh and Y. P. Lysanov, *Fundamentals of Ocean Acoustics*, Springer-Verlag, 2003.

[17] M. Stojanovic, "Underwater acoustic communications: design considerations on the physical layer," *Proceedings of Conference on Wireless on Demand Network Systems and Services*, pp. 1-10, 2008.

[18] C. He, M. Ran, Q. Meng and J. Huang, "Underwater acoustic communications using M-ary chirp-DPSK modulation," *Proceedings of IEEE Conference on Signal Processing*, pp. 1544-1547, 2010.

[19] A. M. Matarneh and S. S. A. Obayya, "Bit-error ratio performance for radio over multimode fibre system using coded orthogonal frequency division multiplexing," *IET Optoelectronics*, vol. 5, no. 4, pp. 151-157, 2011.